Reviewer 1

Li et al. proposed a functionality-based approach to predict the formation of secondary organic aerosol (SOA) from m-xylene photooxidation. Four condensable oxidized organics (COO) with distinct functionalities contributing to m-xylene-derived SOA were quantified by simultaneously measuring gas- and particle-phase components. Interfacial uptake, acid-base reaction, and oligomerization were investigated under 10% and 70% relative humidity. A kinetic model was developed to reproduce SOA formation from m-xylene photooxidation. The manuscript is overall well written, and the data analysis is comprehensive. The topic fits ACP, and the derived parameters (yields and uptake coefficients) will benefit the community. I recommend acceptance after some minor revisions.

We are grateful for the positive and constructive comments to our manuscript by this reviewer and have fully addressed the issues raised by this reviewer below

1. Methodology

I think most of the SI sections can be moved to the main text. ACP has no length limit, and Section 2 should be expanded with details on methods for data analysis, e.g., quantification of products, OH concentration, wall loss, uptake coefficient, model framework, etc.

We have now moved the detailed method information from SI to the main text now. Specifically, we have incorporated the SI methods for **Chamber experiments**, **analytical methods**, **uptake coefficient calculation**, **COO yields**, and **SOA mass concentration and yield** into the **Experimental Methodology section**.

2. Chemical mechanism and model framework

Using P1, P2, and P3 to represent the products is confusing. At first, I thought Pi was a lumped species, but it turned out to be some specific species. Then the questions are: How does P1 connect to P2 in Table S1? For example, there are 2 P1s and 4 P2s, so there will be eight combinations. Which should be used? What are the corresponding differential equations that lead to Eqs S4 - S12? I would use a table to explicitly show the reactions by highlighting species with different colors corresponding to other generations. If possible, list all the differential equations, including all the processes (chemical reactions, particle uptake, and wall loss), before Eqs S4 - S12.

P*i* represents the i^{th} generation products and accounts for the various species detected by ID-CIMS. The formation of P*i* is connected by the chemical mechanism of *m*-xylene photo-oxidation (Figure S2b). We have now clarified this by providing a sentence and a figure for detailed mechanism linking the formation, uptake, and wall loss of P1 to P3, "Note that P_n represents the lumped product of the n^{th} generation, which is related the sequence of OH addition for *m*-xylene photooxidation and accounts for the various species detected by ID-CIMS (Figure S2b)." on p. 14.

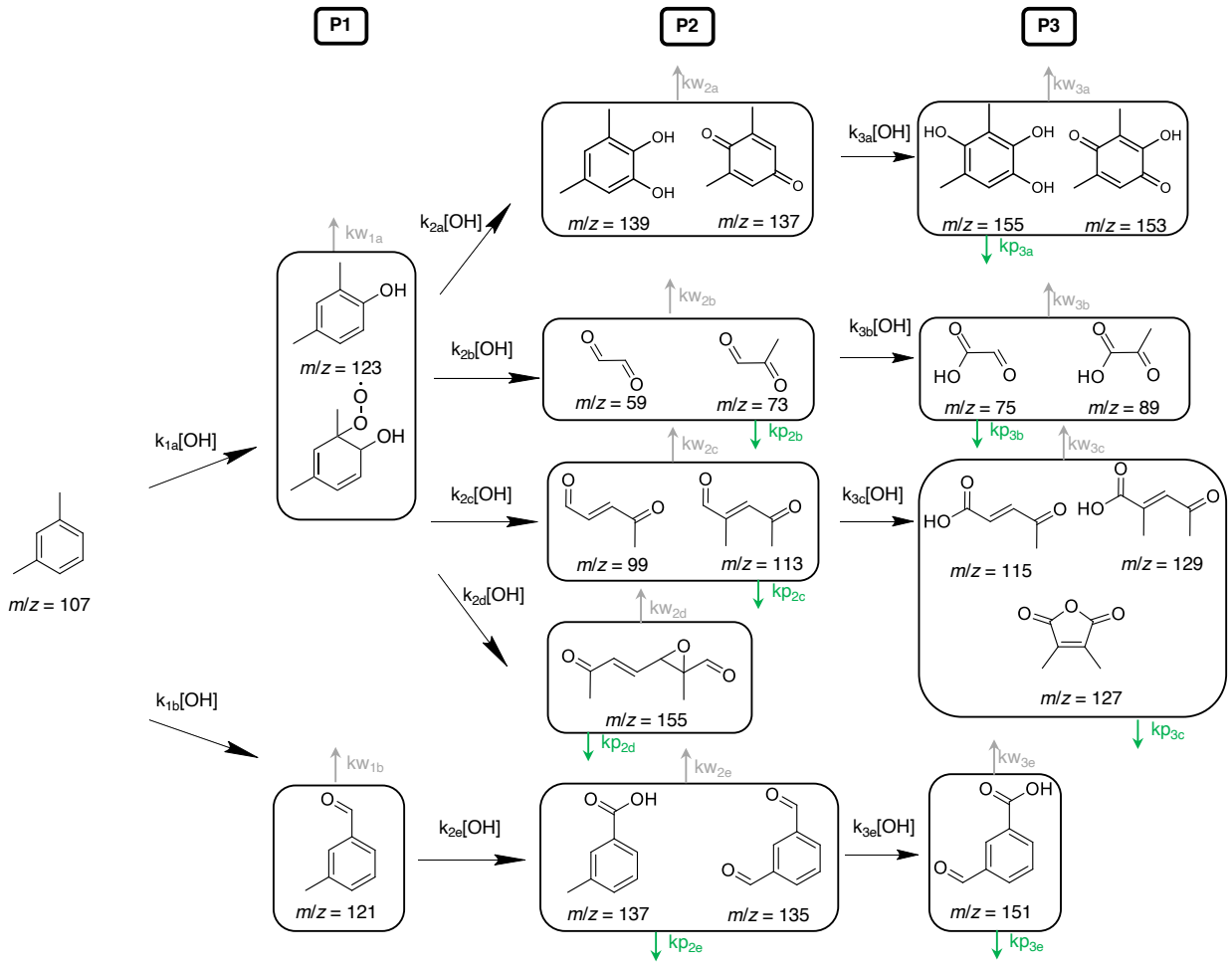

Figure S2b. Multi-generation products from *m*-xylene-OH photooxidation. The letters of P1, P2, and P3 denote the products of first, second, and third generation of reactions with OH, respectively. The species in each box are lumped in the kinetic simulation with their rate constant with OH (k_i), wall loss rate constant (kw_i), and uptake rate constant (kp_i) listed in Table S1. The numbers denote the mass to charge ratio (*m/z*).

3. Eqs 2, S3, and S25 missed the correction factor for non-continuum diffusion and imperfect accommodation (Eq 12.43 in Seinfeld and Pandis 2016), which may lower the derived uptake coefficient. Please correct.

According to Seinfeld and Pandis 2016, the correction factor for non-continuum diffusion and imperfect accommodation (f(Kn, α)) are applied for calculation of mass transfer from gas to particles for a transition regime flow when accommodation coefficient of gas is not unity (α<1). In our study, the measured uptake coefficient for each type of COO (γ_i) is directly derived from the measured particle growth (Eq. 9), which implicitly includes the correction for non-continuum diffusion and imperfect accommodation.

We have now clarified on p. 21, "In our study, the measured uptake coefficient for each type COO (γ_i) is derived from the measured particle growth (eqs. 9 and 10), which implicitly accounts for non-continuum diffusion, imperfect accommodation, and evaporation (Zhang et al., 1994; Ravishankara, 1997)"

Reviewer 3

Overall comment: This work examined the functionality-based SOA formation from m-xylene photooxidation, combining gas-phase composition measurements, aerosol property measurements, and a kinetic simulation. The main conclusion is that the authors categorized the total SOA products into four major functionality-based groups: dicarbonyls, carboxylic acids, polyhydroxy aromatics/quinones, and nitrophenols. Then the authors argued that the parameterized uptake coefficients of the four groups can simulate the SOA mass concentration and concluded that functionality-based approach could extend to the SOA formation from other VOCs as well. However, this conclusion is in strong contrast to the established volatility-based SOA formation understanding. Unfortunately, the authors did not provide convincing evidence for their conclusion. One obvious problem is that evaporation of these products from SOA back to the gas phase is not considered in their model. There are also other technical issues. Thus, the manuscript needs to be revised before consideration for publication.

We thank the reviewer for the constructive comments to improve our manuscript and have revised the manuscript accordingly to account for the reviewer's suggestions.

We have deleted the statement, "the functionality-based approach is broadly applicable to VOC oxidation for other species" in the abstract.

Detailed comments:

1. Line 50 – 57. I think a mechanism figure could help explain the chemical reactions here. Figure 1f helps a little, but I feel a more comprehensive mechanism separately shown is better.

We have provided a mechanism figure Fig. S2a to explain the initial oxidation mechanism of m-xylene.

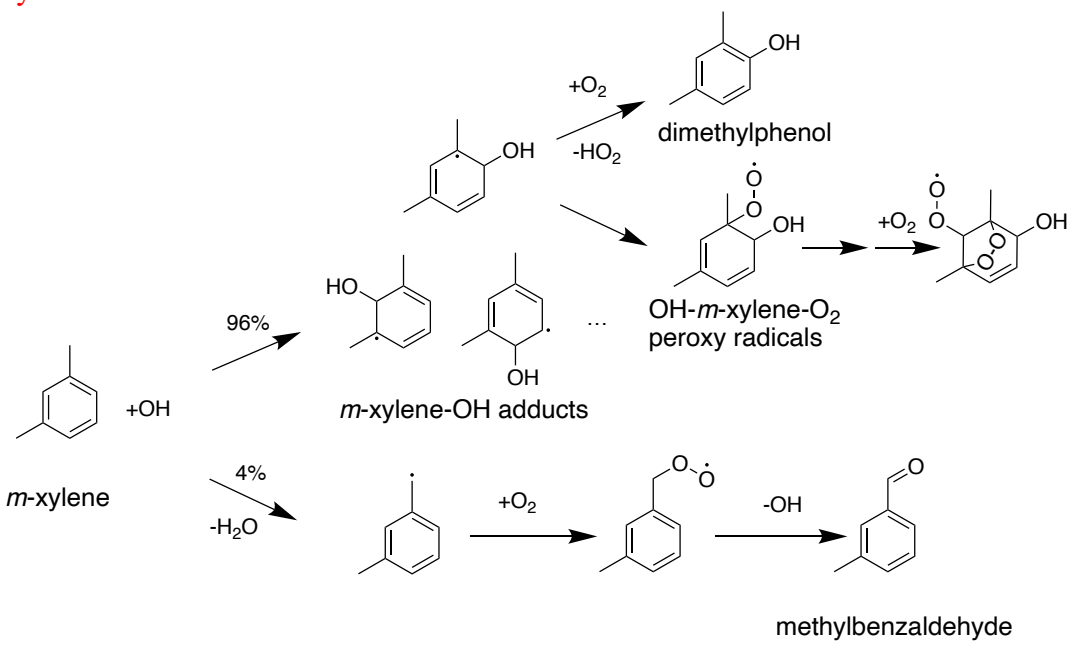

Fig. S2a. The initial oxidation mechanism for OH oxidation of *m*-xylene leading to the formation of m-xylene-OH adducts, dimethylphenol, OH-m-xylene-O_2 peroxy radicals, and methylbenzaldehyde.

2. Line 80 – 84. Although it is true that non-equilibrium processes exist, volatility still dominates the overall gas-particle partitioning process. There have been many, many measurements suggesting that. That the volatility-based approach under-predicts SOA formation does not mean volatility-based idea is wrong. The non-equilibrium processes and particle-phase reactions only make the gas-particle partitioning estimated based on vapor pressure inaccurate in some cases, but overall, volatility is the driving property.

We respectfully disagree with this view of the reviewer, even more so philosophically. Scientific research shall be judged solely based on the available evidence, but not on a prevailing view or one's perception. While the reviewer is correct in pointing out that equilibrium partitioning and volatility-based condensation represent the dominant framework to treat SOA formation in the atmospheric chemistry community, the overwhelming evidence from our work lies in the significant increase in particle size (Fig. 2a) and constantly varying particle properties (i.e., SSA in Fig. 2b and density in Fig. 5c,d), which closely correlate with the gaseous production of condensable oxidized organics (COO) in Fig. 1. These results indicate a highly nonequilibrium kinetic process leading to SOA formation from m-xylene oxidation, which cannot be described by equilibrium partitioning. Also, the direct detection of the particle-phase products confirms that organic acids and dicarbonyls directly participate in the heterogeneous reactions to yield low-volatility products. Moreover, the volatility-based equilibrium partitioning cannot not explain the variations in the particle size growth, SSA, and chemical compositions on different seed particles (Fig. 3). Our work did provide evidence for condensation from low-volatility COO (i.e., polyhydroxy aromatics/quinones, and nitrophenols), but showed the dominant contributions from volatile COO species such as organic acids and dicarbonyls (Fig. 5b). In our study, the vapor pressures of the detected gaseous oxidation products for organic acids and dicarbonyls are too large to explain the measured particle growth via equilibrium partitioning (Table S6). Moreover, the direct detection of the particle-phase products confirms that organic acids and dicarbonyls directly participate in the particle-phase reactions to yield low-volatility products. Specifically, the saturation vapor pressures of organic acids detected in the particle-phase range from 1.9×10^{-3} to 6.6×10^{-6} atm, while their gas-phase concentrations range from 0.5 to 2.5 ppb. Similarly, the saturation vapor pressures of dicarbonyls detected in the particle-phase range from 1.6×10^{-1} to 3.9×10^{-4} atm, while their gas-phase concentrations range from 0.5 to 2.2 ppb. The high saturation vapor pressure and low gas-phase concentrations render equilibrium partitioning of those COOs implausible in our experiments, indicating that the aerosol growth and SOA formation in our study are mainly driven by multiphase reactions of organic acids and dicarbonyls, via acid-base reactions and oligomerization, respectively.

We have now clarified on p. 20, "Our work shows significant increase in particle size (Fig. 2a) and constantly varying particle properties, i.e., SSA (Fig. 2b) and density (Fig. 5c,d), which closely correlate with the gaseous COO production (Fig. 1). These results imply a highly nonequilibrium kinetic process leading to SOA formation from m-xylene oxidation, which cannot be described by equilibrium partitioning. The gas-to-particle conversion from *m*-xylene is dominated by several volatile COO species (i.e., organic acids and dicarbonyls) and with minor contribution from condensation of low-volatility COO (i.e., polyhydroxy aromatics/quinones, and nitrophenols) (Fig. 5b). In our study, the vapor pressures of the detected gaseous oxidation products for organic acids and dicarbonyls are too large to explain the measured particle growth via equilibrium partitioning (Table S6). Specifically, the saturation vapor pressures of organic acids detected in the particle-phase range from 1.9×10^{-3} to 6.6×10^{-6} atm, while their gas-phase concentrations range from 0.5 to 2.5 ppb. Similarly, the saturation vapor pressures of dicarbonyls

detected in the particle-phase range from 1.6×10^{-1} to 3.9×10^{-4} atm, while their gas-phase concentrations range from 0.5 to 2.2 ppb. The high saturation vapor pressures and low gas-phase concentrations for those COOs render equilibrium partitioning implausible in our experiments. Also, the direct detection of the particle-phase products confirms that organic acids and dicarbonyls directly participate in heterogeneous reactions to yield low-volatility products. Moreover, volatility-based equilibrium partitioning cannot not explain the variations in the particle size growth, SSA, and chemical compositions on different seed particles (Fig. 3). Clearly, the gas-to-particle conversion from *m*-xylene oxidation involves several distinct heterogeneous processes, including interfacial attraction, ionic dissociation/acid-base reaction, and nucleophilic oligomerization (Li et al., 2021a,b)"

3. A lot of the details of the experiments and model should be provided in the main text. For example, what is the ion chemistry of the ID-CIMS? What is the mass resolution and if low mass resolution, how were the chemical formulas resolved? How was the thermal desorption carried out? At what temperature for how long? How were the products quantified? What were the uncertainties? How were the product yield quantified? How were the uptake coefficients determined? How was the model developed? These are all very important details to help readers understand the discussion and should move from the supporting information to the main text.
We have moved the necessary supporting information into the main text. Specifically, we have incorporated the SI methods for **Chamber experiments**, **analytical methods**, **uptake coefficient calculation**, **COO yields**, and **SOA mass concentration and yield** into the **Experimental Methodology section**.
Additionally, we have added the following statement on p. 6, "Briefly, the concentration of species A from the proton transfer reaction ($H_3O^+ + A \rightarrow H_2O + HA^+$) is determined by".
We have provided the followings on p. 8, "Seed particles after 20 min of exposure to photooxidation were collected for 2 hours by a platinum filament (with a collection voltage of about 3000 V) in a 2.5 slpm flow from the reaction chamber, and the analytes were evaporated by heating the filament to 350°C for 2 s and detected by ID-CIMS using H_3O^+ as the reagent ions. The mass resolution of TD-ID-CIMS was about 0.5 amu. The desorption signal was represented by the relative intensity (RI) of the integrated peak area during heating. The uncertainties of TD-ID-CIMS measurements arose from the flow rate, voltage, collection time, evaporation voltage, and mass spectrometer ionization/detection efficiencies during particle collection and were represented by the standard deviation of three repeated measurements."

4. The authors claimed that the product identification method does not induce fragmentation. However, it appears that the IT-CIMS is essentially similar to (H3O+) PTR-MS. It is known that PTR-MS does have some fragmentation for some compounds (see Yuan and de Gouw, Chem. Rev. 2017, 117, 13187). How can the authors be certain that the measured ions did not induce fragmentation? Also, thermal desorption was used for SOA composition? Thermal desorption is known to cause fragmentation of species. Could there be fragmentation?
In our work, most of the particle-phase products were assigned to the parent-peaks of organic acids or oligomers for dicarbonyls, indicating little fragmentation from either termal desorption or ionization by H_3O^+. According to Yuan and de Gouw (Chem. Rev. 2017, 117, 13187), the degree of fragmentation is dependent on electric field in drift tube and relative humidity. Fragmentation of most product ions is insignificant when the drift tube in PTR-MS with E/N of 100−120 Td. Moreover, the degrees of fragmentation for many VOCs decrease with higher

humidity. An ion drift tube was used both in our ID-CIMS and TD-ID-CIMS configurations. An electric field of E/N = 138 Td was applied for ID-CIMS at high RH (i.e., 70%) and E/N = 110 Td was used for TD-ID-CIMS setup at low RH (~ 0%). This electric field effectively avoided fragmentation for most products from the proton transfer reactions.
We have now clarified this on p. 9, "In both ID-CIMS and TD-ID-CIMS configurations, an ion drift- tube was used. An electric field of E/N = 138 Td was applied for ID-CIMS at high RH (i.e., 70%), and E/N = 110 Td was used for TD-ID-CIMS at low RH (< 1%). The electric field effectively avoided fragmentation for most products from the proton transfer reactions (Yuan and de Gouw, 2017). All gaseous and particle-phase products were detected at their respective parent-peaks, indicating little fragmentation from either thermal desorption or ionization by H_3O^+. For example, the major molecules detected by TD-CIMS at high RH from m-xylene oxidation were acetal/hemiacetal oligomers, consistent with a previous study showing intact oligomers with thermal desorption (Claflin and Ziemann, 2019)."

5. The experiments involve many different conditions (RH, seeds, NOx, NH3). I suggest adding a table listing all performed experiments and number the experiments. Refer to the numbers in the discussion.
We have now provided a Table 1 to list all experimental conditions and clarified the experimental conditions accordingly throughout our manuscript.

Table 1 Summary of experimental conditions.

	Seed particle	NH_3 concentration (ppb)	NO_x concentration (ppb)	RH
Exp. 1	AS	19	0	70%
Exp. 2	AS	0	0	70%
Exp. 3	ABS	0	0	70%
Exp. 4	NaCl	0	0	70%
Exp. 5	AS	9.5	0	70%
Exp. 6	AS	28.5	0	70%
Exp. 7	ABS	9.5	0	70%
Exp. 8	ABS	19	0	70%
Exp. 9	ABS	28.5	0	70%
Exp. 10	NaCl	9.5	0	70%
Exp. 11	NaCl	19	0	70%
Exp. 12	NaCl	28.5	0	70%
Exp. 13	AS	19	0	10%
Exp. 14	AS	19	0	30%
Exp. 15	AS	19	0	50%
Exp. 16	AS	19	100	70%
Exp. 17	AS	19	300	70%
Exp. 18	AS	19	500	70%

6. Line 156. The absence of HOM could be due to instrument limitation. In fact, some other species may not be well detected under H3O+ mode.

PTR-MS has been shown to have high sensitivities for many hydrocarbons and oxygenated organics with the proton transfer reaction rate constants of (2 to 4) × 10^{-9} cm^3 $molecule^{-1}$ s^{-1} (Zhao and Zhang, 2004), including non-radical oxidation products from *m*-xylene photo-oxidation. The detection limit (defined as 3 times of the ratio of signal to noise) for the oxidation products from *m*-xylene-OH reactions was estimated to be 50 ppt by the ID-CIMS. It is possible that HOMs were not detected due to their low abundance (less than 50 ppt) in our work. Our results for insignificant contribution of HOMs to SOA formation from m-xylene oxidation are consistent with a small yield of HOMs reported in a previous study (Molteni et al., 2018).
We have now clarified on p. 15, "Negligible products relevant to HOMs were detected in our experiments, indicating a minor importance for the self- and cross-reactions of RO_2 compared to the competing reactions between RO_2 and HO_2/NO/RO_2 to form ring-opening products. Our results for insignificant contribution of HOMs to SOA formation from m-xylene oxidation are consistent with a small yield of HOMs reported in a previous study (Molteni et al., 2018)."

7. In the kinetic model, the authors only represent the uptake/condense process and showed some evidence the functionality-based approach could work. However, the desorption/evaporation of the species from SOA to gas-phase unmentioned. As it is well known, the condense process and equation (e.g, eq. S3) is independent of volatility, but volatility determines gas-particle partitioning in controlling the desorption rate. It was not considered in this manuscript.
Please refer to our response to Q2. The overwhelming evidence from this work lies in the significant increase in particle size (Fig. 2a) and constantly varying particle properties (i.e., SSA in Fig. 2b and density in Fig. 5c,d), which closely correlate with the gaseous production of condensable oxidized organics (COO) in Fig. 1. Our results indicate an efficient kinetic process for SOA formation from m-xylene oxidation, while desorption/evaporation of the COO species from SOA to gas-phase is unimportant, as indicated by the rapid and continuous growth of the particles even after 120 min. Furthermore, our measured uptake coefficient for each type of COO (γ_i) is directly derived from the measured growth of the particles after the drying process (Eq. S9), which implicitly includes any reverse process due to desorption or evaporation of the volatile species.
We have stated the following on p. 21, "In our study, the measured uptake coefficient for each COO type (γ_i) is derived from the measured particle growth (eqs. 9 and 10), which implicitly accounts for non-continuum diffusion, imperfect accommodation, and evaporation (Zhang et al., 1994; Ravishankara, 1997)"